Demonstration of 1 → 3 continuous-variable quantum telecloning

Qingwei Wang,[1] Wei Li,[1] Yimiao Wu,[1] Wenxiu Yao,[1] Fan Li,[1] Long Tian,[1,2] Yajun Wang,[1,2] and Yaohui Zheng[1,2,*]

[1]*State Key Laboratory of Quantum Optics and Quantum Optics Devices, Institute of Opto-Electronics, Shanxi University, Taiyuan 030006, People's Republic of China*

[2]*Collaborative Innovation Center of Extreme Optics, Shanxi University, Taiyuan 030006, People's Republic of China*

(Received 19 July 2021; revised 25 August 2021; accepted 3 September 2021; published 22 September 2021)

The distribution of the quantum states to remote receivers is an indispensable technology in quantum communication, quantum networks, and quantum information processing. Perfect distribution does not allow any quantum information loss of the distributed quantum state. Quantum telecloning, which is made up of quantum cloning and quantum teleportation, is a remote quantum information distribution protocol. Here, we experimentally demonstrate unconditional 1 → 3 quantum telecloning of coherent states, and the fidelities of the cloned states are 0.64 ± 0.01, 0.64 ± 0.01, and 0.49 ± 0.01, respectively. No information about the unknown state is lost during the telecloning process by exploiting the quadripartite entangled modes as an auxiliary resource. Deterministic 1 → 3 quantum telecloning has great potential for applications in advanced quantum technology.

DOI: 10.1103/PhysRevA.104.032419

I. INTRODUCTION

Remote state distribution plays an essential role in configuring long-distance quantum communication [1–3], large-scale quantum networks [4–6], and multiuser quantum computation [7]. Because of the limitation set by the quantum no-cloning theorem, an unknown quantum state cannot be perfectly replicated [8]. The no-cloning limit could be overcome at the expense of reducing the success probability [9]. Although cloning operation with perfect fidelity is forbidden in the case of the deterministic condition, approximate cloning can be implemented. The development of advanced quantum technology has driven the proposal and demonstration of massive cloning schemes [10–16], which distribute quantum states to local destinations. Quantum teleportation [17–26] can distribute a quantum state to the remote receiver, breaking the limitation of local distribution, which lacks the capability of point-to-multipoint distribution [27].

To distribute quantum information to multiple remote receivers, the quantum telecloning scheme was proposed [28,29]. As a remote quantum information distribution protocol, quantum telecloning is made up of quantum cloning and quantum teleportation. In quantum telecloning, the unknown quantum state is distributed to multiple remote receivers, each of which gets an approximate cloned state of the distributed quantum state. By utilizing such a protocol, the information encoded in the unknown state is broadcasted to several spatially separated quantum nodes with the assistance of shared quantum entanglement. As an advanced quantum technology, quantum telecloning has been intensively studied [28,30,31] and demonstrated [32] for photonic qubits. Subsequently, the telecloning scheme was theoretically extended to the continuous-variable (CV) domain [29,33,34] and experimentally realized in virtue of tripartite entanglement as an auxiliary resource [35], demonstrating deterministic 1 → 2 quantum telecloning of coherent states with a fidelity of only 0.58 for each cloner. Recently, the protection of quantum telecloning over noise channels with environment-assisted measurement [36] and weak measurement was proposed, and the entanglement of a quantum channel among separated participants can be recovered probabilistically [37]. However, during quantum telecloning, partial quantum information of the input state may be lost from the sender, which is regarded as an imperfect nonlocal distributor of quantum information.

In this paper, we report an experimental demonstration of deterministic 1 → 3 quantum telecloning of coherent states with the assistance of entangled beams. In contrast to the imperfect 1 → 2 quantum telecloning of coherent states using tripartite entanglement [35], an extra cloned state (the phase-conjugate state [38–40] or time-reversal state) is generated without sacrificing the fidelities of two intrinsic cloned states, and the information that may be lost is collected. The two intrinsic cloned states have the same fidelity of 0.64 ± 0.01, beyond the classical limit, and the fidelity of the extra cloned state is 0.49 ± 0.01, almost the same as the classical limit of $1/2$. Subsequently, the Wigner functions of the cloned states are reconstructed with the maximum-likelihood algorithm to evaluate the performance of quantum telecloning [41,42]. In this paper, we demonstrate deterministic 1 → 3 quantum telecloning, which has great potential for applications in advanced quantum technology [43,44].

II. SCHEMATIC AND EXPERIMENTAL SETUP

The protocol of the deterministic 1 → 3 quantum telecloning was proposed in [45] and can be outlined as follows. Quantum states of light can be described by the electromagnetic field annihilation operator $\hat{a} = (\hat{X} + i\hat{Y})/2$, which is expressed in terms of the amplitude $\hat{X}$ and phase $\hat{Y}$

*yhzheng@sxu.edu.cn

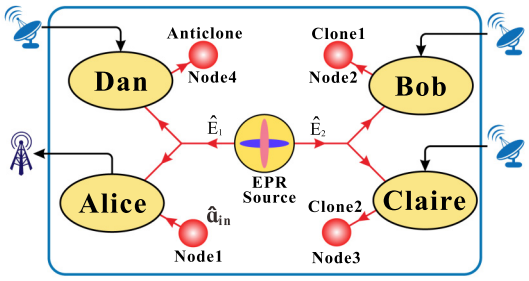

FIG. 1. Schematic diagram of $1 \rightarrow 3$ continuous-variable quantum telecloning. An unknown state from node 1 is distributed to node 2, node 3, and node 4 by using EPR beams as an auxiliary resource. EPR source: Einstein-Podolsky-Rosen entangled beams.

quadratures with the canonical commutator $[\hat{X}, \hat{Y}] = 2i$. The kernel of quantum telecloning is the quantum entanglement shared among the sender and receivers. For the $1 \rightarrow 3$ quantum telecloning depicted in Fig. 1, each submode of Einstein-Podolsky-Rosen (EPR) entanglement is divided into two parts; thus, the quadripartite entangled modes are generated. An unknown state, $\hat{a}_{\rm in}$, is combined with Alice's entangled mode, and the acquired information is then sent to three remote receivers via classical channels. Three remote receivers then reconstruct the initial unknown state with the help of their entangled modes; therefore, the quantum state is distributed to three remote receivers, and no information is lost in the telecloning process. In the ideal case without loss, the restored states at the three receivers' nodes can be expressed as [45]

$$\hat{a}^B_{\rm out} = \hat{a}_{\rm in} + \frac{\sqrt{2}}{2}(\hat{E}_2 - \hat{E}_1^\dagger) + \frac{\sqrt{2}}{2}(\hat{v}_2 - \hat{v}_1^\dagger), \tag{1}$$

$$\hat{a}^C_{\rm out} = \hat{a}_{\rm in} + \frac{\sqrt{2}}{2}(\hat{E}_2 - \hat{E}_1^\dagger) - \frac{\sqrt{2}}{2}(\hat{v}_2 - \hat{v}_1^\dagger), \tag{2}$$

$$\hat{a}^D_{\rm out} = \hat{a}_{\rm in}^\dagger - \sqrt{2}\hat{v}_1, \tag{3}$$

where the superscripts B, C, and D denote receivers Bob, Claire, and Dan. $\hat{E}_1$ and $\hat{E}_2$ are the two submodes of EPR entanglement; $\hat{v}_1$ and $\hat{v}_2$ are the vacuum states introduced by the beam splitters.

Following the above scheme, the experimental setup of $1 \rightarrow 3$ quantum telecloning is shown in Fig. 2. The generation of squeezed fields is based on our earlier experiments presented in [46]. EPR entanglement is generated by combining two independent squeezed beams at a 50:50 beam splitter, with the relative phase $\pi/2$ between the squeezed fields being actively servo controlled. Two optical parametric oscillators (OPOs) with the same parameters operate below the threshold and generate two squeezed fields with wavelengths of 1064 nm. The laser source of our experiment with an output power of 2 W is partly used as the seed beam of two OPOs, the local oscillators for balanced homodyne detection. The remaining light is used for second-harmonic generation to provide the pump field at 532 nm for two OPOs with a threshold of 220 mW. The output power of second-harmonic generation at 532 nm is 1.2 W, which is enough to simultaneously pump two OPOs to produce the entangled state. Based on our previous work, with technical improvements in

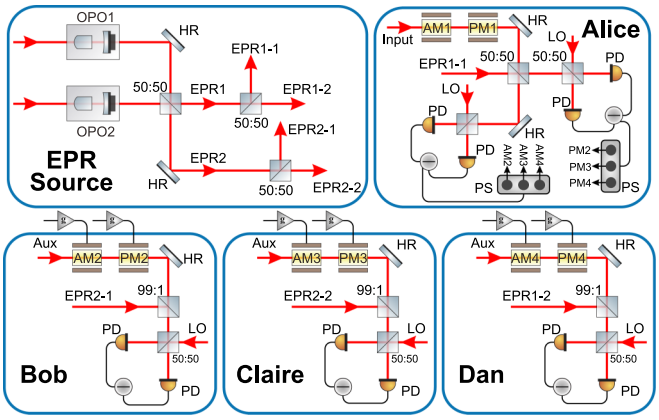

FIG. 2. Experimental setup of $1 \rightarrow 3$ continuous-variable quantum telecloning. OPO, optical parametric oscillator; HR, mirror with a reflectivity larger than 99.95%; AM, amplitude modulator; PM, phase modulator; LO, local oscillator; PD, photodiode; PS, power splitter; Aux, auxiliary beam.

suppressing system loss [46,47], phase noise [48], and detector dark noise [49], the maximum squeezing level is measured to be 13.8 dB below the shot-noise limit (SNL), close to the record level of 15 dB [50]. In the case of $1 \rightarrow 2$ quantum telecloning, only one submode of the EPR beams is divided into two parts by a 50:50 beam splitter to help restore the unknown state at the receiver. When the loss of another submode of EPR beams is less than 50%, it will not decrease the fidelities of the cloned states while inevitably inducing information dropout. By employing another 50:50 beam splitter, information of another submode is utilized to generate the additional cloned state that is the phase-conjugate state (or time-reversal state) without sacrificing the fidelities of two intrinsic cloned states. The scheme not only prevents the information loss of the unknown state but also generates an additional cloned state for quantum information processing [51]. Thus, $1 \rightarrow 3$ quantum telecloning, including two intrinsic cloned states and one extra cloned state, is experimentally realized.

At the sending node (Alice), an amplitude modulator (AM) and a phase modulator (PM) are driven by a function generator at a frequency of 2.0 MHz with a bandwidth of 100 kHz; they are used to set gain factors for the telecloning process. The unknown state is then combined with her entangled mode at a balanced beam splitter to perform a joint measurement. The amplitude and phase quadratures are measured by two balanced homodyne detectors with the assistance of two local oscillators. The extracted information from homodyne detection is divided by the power splitters and then dispatched to the remote receivers through classical channels with proper gain [52,53]. The auxiliary beam at each receiver's terminal acquires the transmitted information with an AM and a PM; a half-wave plate (not shown) placed before the AM and PM is used to eliminate the crosstalk between the AM and PM. In the experiment, the distances between the sender and receivers are about 3 m. At each receiver's terminal, the auxiliary beam with the transmitted information is then combined with the entangled mode at a 99:1 mirror to reassemble the unknown quantum state. A local oscillator is used to perform verification via balanced homodyne detection, the alternating current

signal of which is used to reconstruct the Wigner function with an oscilloscope (not shown) and to obtain the noise power with a spectrum analyzer (not shown) of the reassembled state.

III. EXPERIMENTAL RESULTS AND ANALYSIS

Fidelity $F \equiv \langle\psi_{\text{in}}|\hat{\rho}_{\text{out}}|\psi_{\text{in}}\rangle$, the overlap between the input state $|\psi_{\text{in}}\rangle$ and the output state $|\psi_{\text{out}}\rangle$ with the density matrix $\hat{\rho}_{\text{out}} = |\psi_{\text{out}}\rangle\langle\psi_{\text{out}}|$, is invariably used to evaluate the performance of the cloned state. For an input coherent state, the fidelity can be written as [19]

$$F = \frac{2}{\sqrt{\left(1+\sigma_x^{\text{out}}\right)\left(1+\sigma_y^{\text{out}}\right)}} \tag{4}$$

where σ_x^{out} and σ_y^{out} are the variances of the quadratures of the output state normalized using a coherent state. According to Eqs. (1), (2), and (3), the fidelities of the cloned states at receivers' terminals are obtained as follows:

$$F_B = F_C = \frac{2}{3+e^{-2r}}, \tag{5}$$

$$F_D = \tfrac{1}{2}, \tag{6}$$

where r represents the squeezing factor. For the classical case with $r = 0$, which means there is no EPR correlation, the fidelity of each cloned state at Bob's and Claire's receiving terminals is found to be $1/2$, the same as the classical limit for coherent state cloning. The fidelity of the cloned state at Dan's receiving terminal is always $1/2$, independent of the entangled correlation. Once EPR entanglement is introduced for any $r > 0$, the fidelity of Bob's and Claire's cloning states will exceed the classical limit, which suggests the success of quantum telecloning. Together with the extra cloned state at Dan's terminal, $1 \rightarrow 3$ quantum telecloning is realized. It is worth noting that with infinite squeezing and zero loss, the optimal fidelity of each cloned state at Bob's and Claire's terminal is $2/3$, the same as the no-cloning limit. In our experiment, the quantum efficiency of the diodes is more than 99% [46]; the interference visibility at the homodyning is about 99.8%. After generation, the optical loss (including all the propagation loss and interference imperfections during beam coupling) before homodyne detection is about 6% for nonclassical states. The expected fidelity is about 0.64 according to these imperfections.

To verify the performance of $1 \rightarrow 3$ quantum telecloning, the noise variances of the cloned states are measured. Before the verification, the gain factor is carefully adjusted to ensure the performance of quantum telecloning [52]. The method to keep the unity gain factor is shown in Fig. 3; with an input modulation amplitude of 20 dB, we show the noise power recorded at the sender's and receivers' nodes while scanning the phase of the input beam without EPR correlation. Figure 3(a) shows the noise power of the input quantum state, while Fig. 3(b) shows the noise power recorded by Bob's balanced homodyne detectors. Trace (i) (solid black line) represents the SNL that is obtained with only the local oscillator injecting into the balanced homodyne detectors; trace (ii) (dashed red line) and trace (iii) (dotted blue line) are the amplitude and phase quadratures of the input state [Fig. 3(a)] and reconstructed state [Fig. 3(b)], in which the peak output

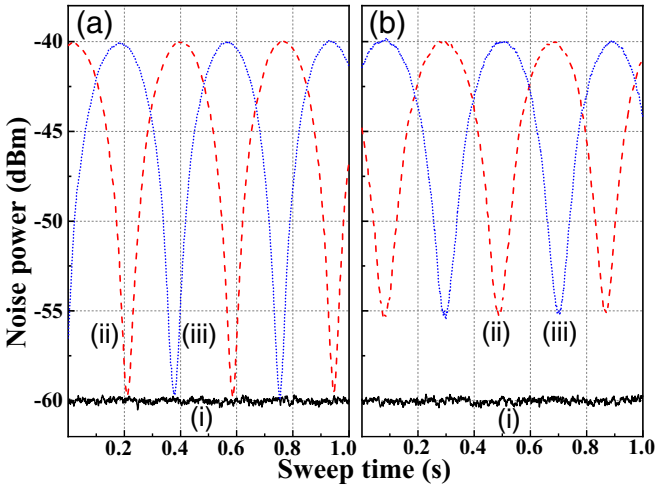

FIG. 3. Noise power recorded while scanning the phase of the input beam without EPR correlation: (a) Noise power of the input quantum state with an input modulation amplitude of 20 dB; trace (i) is the SNL (solid black line), and trace (ii) (dashed red line) and trace (iii) (dotted blue line) are the amplitude and phase quadratures. (b) Noise power recorded by Bob's balanced homodyne detectors; trace (i) is the SNL (solid black line), and trace (ii) (dashed red line) and trace (iii) (dotted blue line) are the reconstruction of a modulation amplitude of 20 dB, showing the same peak output amplitudes as input amplitudes. The noise powers recorded at Claire's and Dan's terminals are the same as Bob's. All the traces are measured via balanced homodyne detection with an analysis frequency of 2.0 MHz.

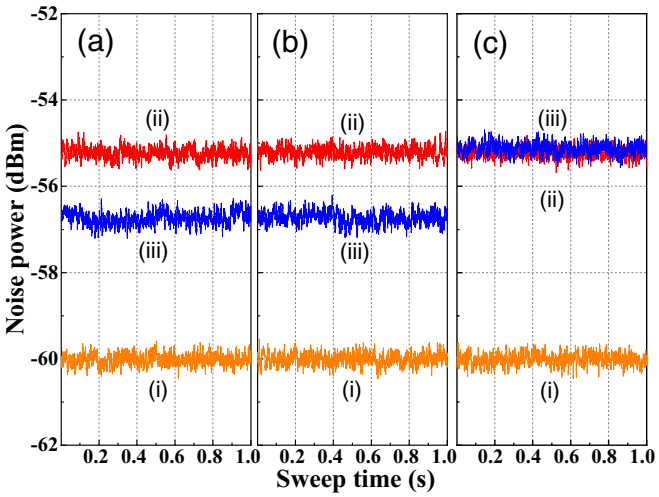

FIG. 4. Noise power of the cloned states with a vacuum input: (a) the cloned state at Bob's terminal, (b) the cloned state at Claire's terminal, and (c) the cloned state at Dan's terminal. Trace (i) [orange (light gray) line] represents the shot-noise limit; trace (ii) [red (medium gray) line] is the noise power of the cloned state without EPR entanglement, and trace (iii) [blue (dark gray) line] expresses the noise power of the cloned state with the help of EPR entanglement. The measured results are the same for amplitude and phase quadratures; only the amplitude quadrature is shown. All the traces are measured via balanced homodyne detection with an analysis frequency of 2.0 MHz.

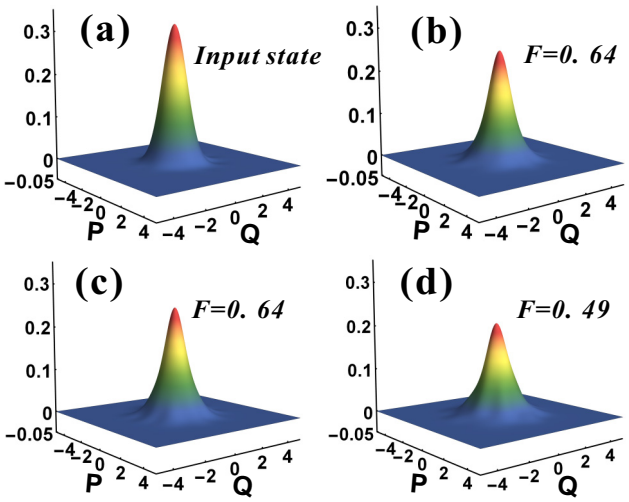

FIG. 5. Reconstructing the Wigner function of the input and cloned states at the sender's and receivers' terminals. (a) Wigner function of the input state at Alice's terminal. (b) Wigner function of the cloned state at Bob's terminal. (c) Wigner function of the cloned state at Claire's terminal. (d) Wigner function of the cloned state at Dan's terminal. P and Q are the momentum and position in phase space.

amplitudes are the same as the input amplitudes. The noise powers recorded at Claire's and Dan's terminals are the same as those at Bob's terminal (not shown). In all measurements the Fourier frequency is 2.0 MHz, the resolution bandwidth is 100 kHz, and the video bandwidth is 100 Hz.

After calibrating the gain factor, the EPR entanglement is used as an auxiliary resource to perform the $1 \rightarrow 3$ quantum telecloning of the coherent state. To show the variances of the cloned states more clearly, the vacuum state is chosen as the input state (the input modulation is canceled) here, and the noise power of the cloned states is shown in Fig. 4. Trace (i) [orange (light gray) line] represents the SNL; trace (ii) [red (medium gray) line] is the noise power of the cloned states without EPR entanglement that represents the classical limit, and trace (iii) [blue (dark gray) line] expresses the noise power of the cloned states with the assistance of EPR entanglement at Bob's [Fig. 4(a)], Claire's [Fig. 4(b)], and Dan's [Fig. 4(c)] terminals. For each cloner, the noise power is about 1.5 dB below trace (ii), 1.5 dB below trace (ii), and 0.1 dB above trace (ii), respectively. According to Eq. (4), the fidelities of the cloned states are calculated to be 0.64 ± 0.01, 0.64 ± 0.01, and 0.49 ± 0.01.

The Wigner function, a quasiprobability distribution of quadrature amplitude and phase in phase space, provides the complete quantum characteristics of a quantum state. The optical homodyne tomography technique is used to reconstruct the density matrix and Wigner function of the quantum state from the experimental data. The alternating current signal of the homodyne detector is mixed with a 500-mV_{pp} sinusoidal signal of 2.0 MHz. Then the resulting signal is filtered by a low-pass filter (the cutoff frequency is 1.9 MHz) and subsequently amplified by a low-noise preamplifier with broadband of 30 kHz and gain of 500 to obtain probability distributions. An oscilloscope (about 1 000 000 points per trace) is used to record the signal for measuring marginal distributions in the temporal mode of the state. The density matrix that maximizes the likelihood of the quantum state is obtained by performing sequential iterations of the recorded data. The Wigner function of the cloned states is reconstructed with the density matrix to quantify the performance of the $1 \rightarrow 3$ quantum telecloning process, which is shown in Fig. 5. Figure 5(a) shows the reconstructed Wigner function of the input state, while Figs. 5(b), 5(c), and 5(d) are the reconstructed Wigner functions of the cloned states at Bob's, Claire's, and Dan's terminals, respectively.

IV. CONCLUSION

In conclusion, we have experimentally demonstrated $1 \rightarrow 3$ quantum telecloning of coherent states with the assistance of quadripartite entangled modes. By reconstructing the extra cloned state without sacrificing the fidelities of two intrinsic cloned states, no information about the distributed state is lost during the telecloning process. The fidelities of the cloned states are 0.64 ± 0.01, 0.64 ± 0.01, and 0.49 ± 0.01, respectively. The Wigner functions of the cloned states were also reconstructed to quantify the performance of the $1 \rightarrow 3$ quantum telecloning. Such telecloning is the deterministic distribution of quantum states to multiple remote nodes, which has great possibilities in long-distance quantum communication and quantum networks.

ACKNOWLEDGMENTS

We acknowledge financial support from the National Natural Science Foundation of China (NSFC; Grants No. 62027821, No. 11654002, No. 11804206, No. 11804207, No. 11874250, No. 62035015), the National Key Research and Development Program of China (Grant No. 2020YFC2200402), the Key Research and Development Projects of Shanxi (Grant No. 201903D111001), the Program for Sanjin Scholar of Shanxi Province, the Program for Outstanding Innovative Teams of Higher Learning Institutions of Shanxi, and the Fund for Shanxi 1331 Project Key Subjects Construction.

[1] S. Muralidharan, J. Kim, N. Lütkenhaus, M. D. Lukin, and L. Jiang, Ultrafast and Fault-Tolerant Quantum Communication Across Long Distances, Phys. Rev. Lett. **112**, 250501 (2014).

[2] F. Ewert, M. Bergmann, and P. V. Loock, Ultrafast Long-Distance Quantum Communication with Static Linear Optics, Phys. Rev. Lett. **117**, 210501 (2016).

[3] S. Shi, L. Tian, Y. Wang, Y. Zheng, C. Xie, and K. Peng, Demonstration of Channel Multiplexing Quantum Communication Exploiting Entangled Sideband Modes, Phys. Rev. Lett. **125**, 070502 (2020).

[4] H. J. Kimble, The quantum internet, Nature (London) **453**, 1023 (2008).

[5] J. I. Cirac, P. Zoller, H. J. Kimble, and H. Mabuchi, Quantum State Transfer and Entanglement Distribution among Distant Nodes in a Quantum Network, Phys. Rev. Lett. **78**, 3221 (1997).

[6] S. L. Braunstein, V. Bužek, and M. Hillery, Quantum-information distributors: Quantum network for symmetric and asymmetric cloning in arbitrary dimension and continuous limit, Phys. Rev. A **63**, 052313 (2001).

[7] S. Lloyd and S. L. Braunstein, Quantum Computation over Continuous Variables, Phys. Rev. Lett. **82**, 1784 (1999).

[8] W. K. Wootters and W. H. Zurek, A single quantum cannot be cloned, Nature (London) **299**, 802 (1982).

[9] J. Y. Haw, J. Zhao, J. Dias, S. M. Assad, M. Bradshaw, R. Blandino, T. Symul, T. C. Ralph and P. K. Lam, Surpassing the no-cloning limit with a heralded hybrid linear amplifier for coherent states, Nat. Commun. **7**, 13222 (2016).

[10] E. Nagali, L. Sansoni, F. Sciarrino, F. D. Martini, L. Marrucci, B. Piccirillo, E. Karimi, and E. Santamato, Optimal quantum cloning of orbital angular momentum photon qubits through Hong-Ou-Mandel coalescence, Nat. Photonics **3**, 720 (2009).

[11] H. Fan, Y. Wang, L. Jing, J. Yuea, H. Shi, Y. Zhang, and L. Mu, Quantum cloning machines and the applications, Phys. Rep. **544**, 241 (2014).

[12] V. Scarani, S. Iblisdir, N. Gisin, and A. Acín, Quantum cloning machines and the applications, Rev. Mod. Phys. **77**, 1225 (2005).

[13] N. Gisin and S. Massar, Optimal Quantum Cloning Machines, Phys. Rev. Lett. **79**, 2153 (1997).

[14] N. J. Cerf, A. Ipe, and X. Rottenberg, Cloning of Continuous Quantum Variables, Phys. Rev. Lett. **85**, 1754 (2000).

[15] S. Liu, Y. Lou, Y. Chen, and J. Jing, All-Optical Optimal N-to-M Quantum Cloning of Coherent States, Phys. Rev. Lett. **126**, 060503 (2021).

[16] L. Peng, D. Wu, H. Zhong, Y. Luo, Y. Li, Y. Hu, X. Jiang, M. Chen, L. Li, N. Liu, K. Nemoto, W. J. Munro, B. C. Sanders, C. Lu, and J. Pan, Cloning of Quantum Entanglement, Phys. Rev. Lett. **125**, 210502 (2020).

[17] C. H. Bennett, G. Brassard, and C. Crépeau, Teleporting an Unknown Quantum State via Dual Classical and Einstein-Podolsky-Rosen Channels, Phys. Rev. Lett. **70**, 1895 (1993).

[18] S. L. Braunstein and H. J. Kimble, Teleportation of Continuous Quantum Variables, Phys. Rev. Lett. **80**, 869 (1998).

[19] A. Furusawa, J. L. Sørensen, S. L. Braunstein, C. A. Fuchs, H. J. Kimble, and E. S. Polzik, Unconditional quantum teleportation, Science **282**, 706 (1998).

[20] D. Bouwmeester, J. Pan, K. Mattle, M. Eibl, H. Weinfurter, and A. Zeilinger, Experimental quantum teleportation, Nature (London) **390**, 575 (1997).

[21] S. Takeda, T. Mizuta, M. Fuwa, P. V. Look, and A. Furusawa, Deterministic quantum teleportation of photonic quantum bits by a hybrid technique, Nature (London) **500**, 315 (2013).

[22] S. Pirandola, J. Eisert, C. Weedbrook, A. Furusawa, and S. L. Braunstein, Advances in quantum teleportation, Nat. Photonics **9**, 641 (2015).

[23] Q. Wang, Y. Tian, W. Li, L. Tian, Y. Wang, and Y. Zheng, High-fidelity quantum teleportation toward cubic phase gates beyond the no-cloning limit, Phys. Rev. A **103**, 062421 (2021).

[24] T. C. Ralph, All-optical quantum teleportation, Opt. Lett. **24**, 348 (1999).

[25] W. P. Bowen, N. Treps, B. C. Buchler, R. Schnabel, T. C. Ralph, H. Bachor, T. Symul, and P. K. Lam, Experimental investigation of continuous-variable quantum teleportation, Phys. Rev. A **67**, 032302 (2003).

[26] N. Takei, H. Yonezawa, T. Aoki, and A. Furusawa, High-Fidelity Teleportation beyond the No-Cloning Limit and Entanglement Swapping for Continuous Variables, Phys. Rev. Lett. **94**, 220502 (2005).

[27] Q. Wang, Y. Wang, X. Sun, Y. Tian, W. Li, L. Tian, X. Yu, J. Zhang, and Y. Zheng, Controllable continuous variable quantum state distributor, Opt. Lett. **46**, 1844 (2021).

[28] M. Murao, D. Jonathan, M. B. Plenio, and V. Vedral, Quantum telecloning and multiparticle entanglement, Phys. Rev. A **59**, 156 (1999).

[29] P. van Loock and S. L. Braunstein, Telecloning of Continuous Quantum Variables, Phys. Rev. Lett. **87**, 247901 (2001).

[30] I. Ghiu and A. Karlsson, Broadcasting of entanglement at a distance using linear optics and telecloning of entanglement, Phys. Rev. A **72**, 032331 (2005).

[31] X. Wang and G. Yang, Hybrid economical telecloning of equatorial qubits and generation of multipartite entanglement, Phys. Rev. A **79**, 062315 (2009).

[32] Z. Zhao, A. N. Zhang, X. Q. Zhou, Y. A. Chen, C. Y. Lu, A. Karlsson, and J. W. Pan, Experimental Realization of Optimal Asymmetric Cloning and Telecloning via Partial Teleportation, Phys. Rev. Lett. **95**, 030502 (2005).

[33] A. Ferraro and M. G. A. Paris, Multimode entanglement and telecloning in a noisy environment, Phys. Rev. A **72**, 032312 (2005).

[34] J. Zhang, C. Xie, K. Peng, and P. van Loock, Continuous-variable telecloning with phase-conjugate inputs, Phys. Rev. A **77**, 022316 (2008).

[35] S. Koike, H. Takahashi, H. Yonezawa, N. Takei, S. L. Braunstein, T. Aoki, and A. Furusawa, Demonstration of Quantum Telecloning of Optical Coherent States, Phys. Rev. Lett. **96**, 060504 (2006).

[36] M. Sabuncu, R. Filip, G Leuchs, and U. L. Andersen, Environment-assisted quantum-information correction for continuous variables, Phys. Rev. A **81**, 012325 (2010).

[37] H.-J. Wu, Z. Jin, and A.-D. Zhu, Protection of telecloning over noisy channels with environment-assisted measurements and weak measurements, Int. J. Theor. Phys. **57**, 1235 (2018).

[38] N. J. Cerf and S. Iblisdir, Quantum Cloning Machines with Phase-Conjugate Input Modes, Phys. Rev. Lett. **87**, 247903 (2001).

[39] J. Sabuncu, U. L. Andersen, and G. Leuchs, Experimental Demonstration of Continuous Variable Cloning with Phase-Conjugate Inputs, Phys. Rev. Lett. **98**, 170503 (2007).

[40] N. J. Cerf and S. Iblisdir, Phase conjugation of continuous quantum variables, Phys. Rev. A **64**, 032307 (2001).

[41] D. T. Smithey, M. Beck, M. G. Raymer, and A. Faridani, Measurement of the Wigner Distribution and the Density Matrix of a Light Mode using Optical Homodyne Tomography: Application to Squeezed States and the Vacuum, Phys. Rev. Lett. **70**, 1244 (1993).

[42] A. I. Lvovsky and M. G. Raymer, Continuous-variable optical quantum-state tomography, Rev. Mod. Phys. **81**, 299 (2009).

[43] S. L. Braunstein and P. van Loock, Quantum information with continuous variables, Rev. Mod. Phys. **77**, 513 (2005).

[44] M. Ricci, F. Sciarrino, N. J. Cerf, R. Filip, J. Fiurášek, and F. De Martini, Separating the Classical and Quantum

Information via Quantum Cloning, Phys. Rev. Lett. **95**, 090504 (2005).

[45] J. Zhang, C. Xie, and K. Peng, Continuous-variable quantum-information distributor: Reversible telecloning, Phys. Rev. A **73**, 042315 (2006).

[46] W. Yang, S. Shi, Y. Wang, W. Ma, Y. Zheng, and K. Peng, Detection of stably bright squeezed light with the quantum noise reduction of 12.6 dB by mutually compensating the phase fluctuations, Opt. Lett. **42**, 4553 (2017).

[47] K. McKenzie, N. Grosse, W. P. Bowen, S. E. Whitcomb, M. B. Gray, D. E. McClelland, and P. K. Lam, Squeezing in the Audio Gravitational-Wave Detection Band, Phys. Rev. Lett. **93**, 161105 (2004).

[48] S. Shi, Y. Wang, W. Yang, Y. Zheng, and K. Peng, Detection and perfect fitting of 13.2 dB squeezed vacuum states by considering green-light-induced infrared absorption, Opt. Lett. **43**, 5411 (2018).

[49] X. Sun, Y. Wang, L. Tian, Y. Zheng, and K. Peng, Detection of 13.8 dB squeezed vacuum states by optimizing the interference efficiency and gain of balanced homodyne detection, Chin. Opt. Lett. **17**, 072701 (2019).

[50] H. Vahlbruch, M. Mehmet, K. Danzmann, and R. Schnabel, Detection of 15 dB Squeezed States of Light and Their Application for the Absolute Calibration of Photoelectric Quantum Efficiency, Phys. Rev. Lett. **117**, 110801 (2016).

[51] M. Lassen, L. S. Madsen, M. Sabuncu, R. Filip, and U. L. Andersen, Experimental demonstration of squeezed-state quantum averaging, Phys. Rev. A **82**, 021801(R) (2010).

[52] T. C. Zhang, K. W. Goh, C. W. Chou, P. Lodahl, and H. J. Kimble, Quantum teleportation of light beams, Phys. Rev. A **67**, 033802 (2003).

[53] M. Sabuncu, L. Mišta, Jr., J. Fiurášek, R. Filip, G. Leuchs, and U. L. Andersen, Nonunity gain minimal-disturbance measurement, Phys. Rev. A **76**, 032309 (2007).